Robotica: (2020) volume 38, pp. 171–184. © Cambridge University Press 2019
doi:10.1017/S0263574719000547

Addressing Control Implementation Issues in Robotic Systems Using Adaptive Control

Rameez Hayat†‡*, Marion Leibold† and Martin Buss†‡

†*Chair of Automatic Control Engineering, Department of Electrical and Computer Engineering, Technical University of Munich, Theresienstr. 90, 80333, Munich, Germany*
E-mail: marion.leibold@tum.de
‡*TUM Institute of Advanced Study, Technical University of Munich, Lichtenbergstrasse 2a, 85748 Garching, Germany*
E-mail: mb@tum.de

(Accepted March 25, 2019. First published online: May 14, 2019)

SUMMARY
This paper addresses three control implementation issues for trajectory tracking of robotic manipulators: unmodeled dynamics, unknown input saturation and peaking effects during the transient phase. A model-free first-order robust-adaptive control method is used to deal with the unmodeled dynamics. Robust optimality and stability of the controller are proved using the $\mathcal{H}_\infty$ technique and the game-algebraic Riccati equation. An intuitive approach is devised to incorporate the unknown input saturation by modifying the speed of the desired trajectory. The trajectory scaling is performed by using only the state errors. Furthermore, two different techniques are utilized to suppress peaking during the transient response of the trajectory tracking. The first method adds an extra term in the input while the second method uses variable gain to improve the transient response. A systematic procedure for finding the controller parameters is formulated using features, such as rise time and settling time. A three-degree-of-freedom robot manipulator is used for the validation of the proposed controller in simulations and experiments.

KEYWORDS: $\mathcal{H}_\infty$ optimal control; Input-to-state stability; Adaptive control; Orbital stability; Computed torque; Euler–Lagrange.

1. Introduction

Robot manipulators are extensively utilized in industry for high-speed performance. Controlling a robot with high speed and accuracy is still a challenging task. A few of the reasons are the highly coupled nonlinear dynamics, complex friction characteristics, torque saturation and load variation. In addition, there are control implementation issues because of input saturation, unmodeled dynamics and controller tuning. Furthermore, unpredictability at the transient response, especially in adaptive control, is often deteriorating safety. Several types of controllers have been proposed to achieve better performance in terms of state errors, for example, adaptive control,[3,8–10,26,30] robust control,[5–7,19,28] orbital stable control,[1,11] sliding mode control,[2] Generalised proportional integral (GPI) control approach[31] and Active disturbance rejection control (ADRC)[32]. In part, adaptive control is a well-established technique for the control of a robotic manipulator because it requires little information about the system dynamics and guarantees the stability of the closed loop in the presence of bounded disturbances.

* Corresponding author. E-mail: rameez.hayat@tum.de

https://doi.org/10.1017/S0263574719000547 Published online by Cambridge University Press

Several controllers have been proposed to address the implementation issues. Almost all of the state-of-the-art trajectory tracking controllers do not consider input saturation, although saturation decisively affects the performance of the control system in terms of state errors. The input constraints are usually state dependent and uncertain, which makes it difficult to include them in the control loop. One way of considering input constraints is to adjust the speed of the reference path such that the required inputs are within the allowed range. Such approaches are called time-optimal path tracking.[12] Bobrow et al.[13] showed different techniques to find the minimum or optimal time for the tracking of the end effector, while satisfying the input constraints. The optimal time for the reference trajectory is usually evaluated from the inverse dynamics of the manipulator, which allows to find the maximum allowed joint acceleration under the permitted torques. The speed of the trajectory is adjusted according to the maximum joint acceleration; however, these techniques require information about the input constraints and the system model for the inverse dynamics. Usually one of the design objectives is that the end effector follows the desired trajectory even if time is compromised. An approach to include the input constraints by using time scaling is proposed by Shiriaev et al.[1,11] This method focuses on the orbital stability of the desired path. The technique converts the system dynamics into a transverse dynamics using a moving Poincaré section.[20] Any trajectory starting in the vicinity of the desired periodic solution is forced to follow the desired trajectory. In orbital stability, the primary objective is to ensure that the closed-loop system converges to an orbit of the desired trajectory rather than considering the stability as a function of time. But again, the design of such a controller requires an estimated model and information about the time-varying input constraints. Furthermore, for constant input constraints, Lewis et al.[23] proposed a technique that uses online $\mathcal{H}_\infty$ control. This technique uses a quasi-norm to transform the constrained control problem to an unconstrained problem. Ahanda et al.[27] proposed an adaptive back-stepping approach, applied on a manipulator using a support vector machine. The controller is robust to system uncertainties and external disturbances. The abovementioned techniques require that the input constraints are known. Unfortunately, input constraints are not easy to estimate because of many reasons. For example, torque saturation varies with joint velocity because of back electromotive force in the motors, the motors have a maximum voltage rating that limits the maximum current, the drives have gain uncertainty and also there is always some offset.

The next issue in control implementation is to ensure safety during the transient phase. In theory, it is feasible to use a high-gain adaptive controller for fast convergence. But this leads to peaking effects[14] because of the large initial state error and high controller gain. Furthermore, there is high-frequency noise which is partially suppressed by the intrinsic property of motor drives that act as low-pass filters. One of the remedies is to choose a trade-off between fast response and high performance by selecting mid-range values for the control parameters. Another important issue is the tuning of the controller parameters. Tuning is a complicated task,[4,8] and in some cases, it is not desirable to tune the controller by trial-and-error method. A detailed discussion about controllers tuning is given in Hayat et al.[4]

The objective of this paper is the use of a model-free robust-adaptive controller that (a) gives an improved transient and steady-state response by incorporating unknown input saturation, (b) reduces the peaking effect during the transient phase, (c) provides robustness of the system under parameter variations and (d) allows intuitive tuning of the control parameters. A second-order robust-adaptive controller was proposed in our previous work.[4] As a first contribution, we present a simpler first-order version of this robust-adaptive controller with robust optimality and stability proofs. The advantage of the first-order controller is the ease of implementation and avoiding high-frequency noise. Two-players zero-sum game theory[25] is used to form a performance index (PI) that must be minimized and maximized with respect to inputs and disturbances, respectively. $\mathcal{H}_\infty$ optimality is used to perform the analysis, where an inverse-optimal approach is applied to find the PI for the given adaptive controller.

This adaptive controller allows for a performance analysis in terms of the state errors. This means, in steady state, the error only exceeds the maximum allowed value if there is input saturation. The second contribution of this paper is the introduction of a trajectory-scaling formulation that modifies the desired trajectory depending on the input saturation. The desired trajectory is modified only when the motor drives are unable to generate the required torques for the nominal trajectory. The advantage of the proposed method is that no constraints information is required and only states are

https://doi.org/10.1017/S0263574719000547 Published online by Cambridge University Press

used in the feedback loop. The proposed trajectory scaling is only applicable for controllers that offer quantitative performance at steady state.

For an improved transient response, and to avoid peaking without compromising the performance of the system, two techniques are presented in this paper. The first procedure adds an extra term to the controller that is a filtered value of the system states.[24] The second method uses the well-known gain-scheduling technique to improve the transient response. An analytical expression is introduced that modifies the controller gains to avoid peaking during transient phase by using only the state error.

Finally, the adaptive control[3] parameters can be evaluated with little information requirements, for example, rise time, settling time and maximum allowed steady-state error.[29] In general, most of the state-of-the-art controllers have no tuning mechanism.[4] Tuning by trial and error might not be a feasible solution for experiments because of safety issues. The fourth contribution is the evaluation of the control parameters for the adaptive controller using performance limitations.

The rest of the paper is organized as follows: Section 2 explains prerequisites required for the proposed techniques. Section 3 covers the contributions of the article. The validation of the proposed techniques using simulations and experiments is presented in Section 4. Conclusions are drawn in Section 5.

2. Background on the Adaptive Controller

With ease of implementation in mind, we introduce a first-order version of a robust-adaptive controller introduced in our previous work.[3,4] An advantage of the first-order controller is the use of few control parameters compared to the higher-order adaptive control. In Section 3, rigorous stability and robustness proofs are performed for the first-order adaptive controller. We start with a brief introduction to feedback linearization for robotic manipulators, also known as computed-torque or inverse-dynamics controller that is later needed to motivate the first-order robust-adaptive controller.

2.1. Computed torque

Feedback linearization can be utilized to design a proportional derivative (PD) controller for a robotic system with known dynamical parameters. The system dynamics for an n-link manipulator is represented using Euler–Lagrange equations:

$$\boldsymbol{M}(\boldsymbol{q})\ddot{\boldsymbol{q}} + \boldsymbol{C}(\boldsymbol{q}, \dot{\boldsymbol{q}})\dot{\boldsymbol{q}} + \boldsymbol{G}(\boldsymbol{q}) + \boldsymbol{F}(\boldsymbol{q}, \dot{\boldsymbol{q}}) = \boldsymbol{\tau}_{\text{in}} + \boldsymbol{\tau}_{\text{d}}, \tag{1}$$

where $\boldsymbol{M}(\boldsymbol{q}) \in \mathbb{R}^{n\times n}$ is a symmetric positive definite inertia matrix, $\boldsymbol{C}(\boldsymbol{q}, \dot{\boldsymbol{q}}) \in \mathbb{R}^{n\times 1}$ is a vector of Coriolis and centrifugal effects, $\boldsymbol{G} \in \mathbb{R}^{n\times 1}$ consists of the gravitational terms acting on the robot, $\boldsymbol{F} \in \mathbb{R}^{n\times 1}$ is a vector representing friction, $\boldsymbol{q} \in \mathbb{R}^{n\times 1}$ is a vector of joint-angles and $\boldsymbol{\tau}_{\text{in}}$ and $\boldsymbol{\tau}_{\text{d}}$ are vectors of the fully actuated input torques and disturbances applied at each joint, respectively.

For the purpose of feedback linearization, the input torques are chosen such that they cancel all the nonlinearities.[15] Thus

$$\boldsymbol{\tau} = \hat{\boldsymbol{M}}\left(\ddot{\boldsymbol{q}}_{\text{d}} - \boldsymbol{K}_{\text{d}}\dot{\boldsymbol{e}} - \boldsymbol{K}_{\text{p}}\boldsymbol{e}\right) + \hat{\boldsymbol{C}}(\boldsymbol{q}, \dot{\boldsymbol{q}})\dot{\boldsymbol{q}} + \hat{\boldsymbol{G}}(\boldsymbol{q}) + \hat{\boldsymbol{F}}(\boldsymbol{q}, \dot{\boldsymbol{q}}), \tag{2}$$

where $\hat{(\cdot)}$ represents the estimated value, $\boldsymbol{K}_{\text{d}}$ and $\boldsymbol{K}_{\text{p}}$ are the PD gains of the controller, $\boldsymbol{e} = \boldsymbol{q} - \boldsymbol{q}_{\text{d}}$ and $\boldsymbol{q}_{\text{d}}$ is the vector of desired joint angles. In an ideal scenario when there is no disturbance and the system dynamics are known, the above equation reduces to

$$\ddot{\boldsymbol{e}} + \boldsymbol{K}_d\dot{\boldsymbol{e}} + \boldsymbol{K}_p\boldsymbol{e} = \boldsymbol{0}, \tag{3}$$

where $\boldsymbol{e}^* = \boldsymbol{0}$ is a stable equilibrium point for appropriate values of $\boldsymbol{K}_{\text{d}}$ and $\boldsymbol{K}_{\text{p}}$. The controller (2) results in a Lyapunov stable system even if the estimated model is not the exact representation of the real system[15] – however, the performance might be deteriorated.

2.2. Adaptive control

The first-order adaptive controller[3,4] is a model-free control method with only three tuning parameters. One parameter is used to remove the mismatch between the estimated and the real system dynamics. The other two parameters are used to achieve the desired response.

Let

$$\phi = \boldsymbol{M}(\boldsymbol{q})\ddot{\boldsymbol{q}} + \boldsymbol{N}(\boldsymbol{q}, \dot{\boldsymbol{q}}) + \boldsymbol{F}(\boldsymbol{q}, \dot{\boldsymbol{q}}) - \ddot{\boldsymbol{q}} - \boldsymbol{\tau}_{\text{d}}. \tag{4}$$

https://doi.org/10.1017/S0263574719000547 Published online by Cambridge University Press

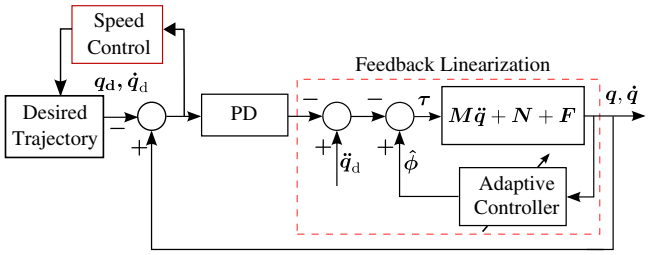


Fig. 1. Adaptive control with speed adjustment.

If we choose

$$\boldsymbol{\tau}_{\text{in}} = \hat{\boldsymbol{\phi}} + \ddot{\boldsymbol{q}}_{\text{d}} - \boldsymbol{K}_{\text{d}}\dot{\boldsymbol{e}} - \boldsymbol{K}_{\text{p}}\boldsymbol{e}, \tag{5}$$

where $\hat{\phi}$ is the estimate of ϕ, then for the system (1), we get the error dynamics

$$\ddot{\boldsymbol{e}} + \boldsymbol{K}_{\text{d}}\dot{\boldsymbol{e}} + \boldsymbol{K}_{\text{p}}\boldsymbol{e} = \hat{\boldsymbol{\phi}} - \boldsymbol{\phi}. \tag{6}$$

The advantage of considering a dynamical vector ϕ that consists of all the system dynamics and the disturbance is that the feedback linearization will not require the individual information about $\boldsymbol{M}$, $\boldsymbol{N}$, $\boldsymbol{G}$ and $\boldsymbol{F}$. To find the input torques in Eq. (5), the proposed adaptive controller is[3]

$$\hat{\boldsymbol{\phi}} = -a\left(\dot{\boldsymbol{e}} + \boldsymbol{K}_{\text{d}}\boldsymbol{e} + \boldsymbol{K}_{\text{p}}\int \boldsymbol{e}\, dt\right). \tag{7}$$

In the next section, we consider Eq. (6) as our new system representation with Eq. (7) as the adaptive controller. The only parameters used in the controller are a, $\boldsymbol{K}_{\text{d}}$ and $\boldsymbol{K}_{\text{p}}$. The parameter '$a$' serves the purpose of feedback linearization, while $\boldsymbol{K}_{\text{p}}$ and $\boldsymbol{K}_{\text{d}}$ are the PD gains for the adaptive controller. Later, an intuitive approach is used to identify the minimum allowed values for the control parameters.

3. Contribution

The contributions of the paper are presented in four parts:

- Robustness and stability of the first-order adaptive controller (7) – see Section 3.1.
- Compensation for unknown input saturation to improve the steady-state response – see Section 3.2.
- Improvement of transient response – see Section 3.3.
- Controller parameters' tuning – see Section 3.4.

As shown in Fig. 1, the proposed controller has three feedback loops. The inner loop in the 'Feedback Linearization' removes the mismatch in the estimation of ϕ. By considering a high value for the controller gain 'a', the mismatch will vanish quickly.[3] Once the vector $\hat{\phi} \to \phi$, the outer loop will achieve the desired specification by tuning the PD gains $\boldsymbol{K}_{\text{d}}$ and $\boldsymbol{K}_{\text{p}}$.

To follow the desired trajectory, the controller might require input that are higher than the maximum allowed torques. Unfortunately, it is not easy to identify the bounds for input torques, so a third loop is devised 'Speed Control' that will modify the speed of the desired trajectory whenever the end effector moves away from the predefined vicinity of the desired path. Finally, an intuitive approach is given to find the controller parameters after finding the minimum allowed values.

3.1. Robust optimality and stability

Before we proof robustness of the control systems (6) and (7), we start with a brief introduction of game-algebraic Riccati and Hamilton–Jacobi–Isaacs equations using the $\mathcal{H}_\infty$ optimality approach. Let a system be given in the state-space form as

$$\dot{\boldsymbol{x}} = \boldsymbol{A}\boldsymbol{x} + \boldsymbol{B}\boldsymbol{u} + \boldsymbol{D}\boldsymbol{d}, \tag{8}$$

https://doi.org/10.1017/S0263574719000547 Published online by Cambridge University Press

where $\boldsymbol{x}, \boldsymbol{A}, \boldsymbol{u}$ and $\boldsymbol{d}$ are the states, transition matrix, input and disturbance, respectively. The $\mathcal{H}_\infty$ PI is

$$V(\boldsymbol{x}) = \min_{\boldsymbol{u}} \max_{\boldsymbol{d}} \int_{\tau}^{\infty} \left(\boldsymbol{x}^T \boldsymbol{Q} \boldsymbol{x} + \boldsymbol{u}^T \boldsymbol{R} \boldsymbol{u} - \gamma^2 ||\boldsymbol{d}||^2\right) dt. \tag{9}$$

The matrices $\boldsymbol{Q}$ and $\boldsymbol{R}$ are positive definite and $\gamma > 0$ is the sensitivity of the system with respect to the disturbance. The above optimal min-max control problem is also called two-players zero-sum problem, where one player ($\boldsymbol{u}$) tries to minimize the cost function, and the other player ($\boldsymbol{d}$) tries to maximize it.[16] The input to the system (8) that results in an optimal solution is

$$\boldsymbol{u}^* = -\boldsymbol{R}^{-1} \boldsymbol{B}^T \boldsymbol{S} \boldsymbol{x} \triangleq -\boldsymbol{K} \boldsymbol{x}. \tag{10}$$

Considering the worst-case disturbance, the game-algebraic Riccati equations for the system is

$$\boldsymbol{A}^T \boldsymbol{S} + \boldsymbol{S} \boldsymbol{A} - \boldsymbol{S} \boldsymbol{B} \boldsymbol{R}^{-1} \boldsymbol{B}^T \boldsymbol{S} + 1/\gamma^2 \boldsymbol{S} \boldsymbol{D} \boldsymbol{D}^T \boldsymbol{S} + \boldsymbol{Q} = \boldsymbol{0}. \tag{11}$$

In the following, we use an inverse optimal approach to determine weighting matrices $\boldsymbol{Q}$, $\boldsymbol{S}$ and $\boldsymbol{R}$ given the controller (7) for (6).

Theorem 1. ***Robustness****: The controller* (7) *for the error dynamics* (6) *is a robust* $\mathcal{H}_\infty$ *control with the performance index* (9)*, if*

$$\boldsymbol{Q} = \begin{bmatrix} \tilde{\boldsymbol{K}} \boldsymbol{K}_{\mathrm{p}}^2 & \boldsymbol{0} & \boldsymbol{0} \\ \boldsymbol{0} & \tilde{\boldsymbol{K}} (\boldsymbol{K}_d^2 - 2\boldsymbol{K}_{\mathrm{p}}) & \boldsymbol{0} \\ \boldsymbol{0} & \boldsymbol{0} & \tilde{\boldsymbol{K}} \end{bmatrix}, \quad \tilde{\boldsymbol{K}} > \boldsymbol{0}. \tag{12}$$

Proof. To rewrite Eqs. (6) and (7) in the forms (8) and (10), let $\boldsymbol{u} = \hat{\phi}$, $\boldsymbol{d} = -\phi$, $\boldsymbol{D} = \boldsymbol{B}$ and $\boldsymbol{x} = [\int \boldsymbol{e}^T dt \quad \boldsymbol{e}^T \quad \dot{\boldsymbol{e}}^T]^T \in \mathbb{R}^{3n \times 1}$. As a consequence,

$$\boldsymbol{A} = \begin{bmatrix} \boldsymbol{0} & \boldsymbol{I} & \boldsymbol{0} \\ \boldsymbol{0} & \boldsymbol{0} & \boldsymbol{I} \\ \boldsymbol{0} & -\boldsymbol{K}_{\mathrm{p}} & -\boldsymbol{K}_{\mathrm{d}} \end{bmatrix} \in \mathbb{R}^{3n \times 3n}, \qquad \boldsymbol{B} = \begin{bmatrix} \boldsymbol{0} \\ \boldsymbol{0} \\ \boldsymbol{I} \end{bmatrix} \in \mathbb{R}^{3n \times 1}.$$

The control input (7) can be written as

$$\hat{\phi} = -a \begin{bmatrix} \boldsymbol{K}_{\mathrm{p}} & \boldsymbol{K}_{\mathrm{d}} & \boldsymbol{I} \end{bmatrix} \begin{bmatrix} \int \boldsymbol{e} dt \\ \boldsymbol{e} \\ \dot{\boldsymbol{e}} \end{bmatrix} \triangleq -\boldsymbol{K} \boldsymbol{x}. \tag{13}$$

From $\boldsymbol{K}$ defined in Eq. (13), using the inverse optimal control technique, the matrices $\boldsymbol{S}$ and $\boldsymbol{Q}$ can be evaluated by Eqs. (10) and (11). With the assumption that $\boldsymbol{Q}$ is a diagonal matrix, we obtain Eq. (12) and

$$\boldsymbol{S} = \begin{bmatrix} \boldsymbol{K}_{\mathrm{p}}^2 + \tilde{\boldsymbol{K}} \boldsymbol{K}_{\mathrm{p}} \boldsymbol{K}_{\mathrm{d}} & \tilde{\boldsymbol{K}} \boldsymbol{K}_{\mathrm{p}} + \boldsymbol{K}_{\mathrm{p}} \boldsymbol{K}_{\mathrm{d}} & \boldsymbol{K}_{\mathrm{p}} \\ \tilde{\boldsymbol{K}} \boldsymbol{K}_{\mathrm{p}} + \boldsymbol{K}_{\mathrm{p}} \boldsymbol{K}_{\mathrm{d}} & \boldsymbol{K}_{\mathrm{d}}^2 + \tilde{\boldsymbol{K}} \boldsymbol{K}_{\mathrm{d}} & \boldsymbol{K}_{\mathrm{d}} \\ \boldsymbol{K}_{\mathrm{p}} & \boldsymbol{K}_{\mathrm{d}} & \boldsymbol{I} \end{bmatrix}. \tag{14}$$

Remark 1. The matrix

$$\boldsymbol{R}^{-1} = \alpha \tilde{\boldsymbol{K}} + \boldsymbol{I}/\gamma^2 \triangleq a \boldsymbol{I}, \quad \alpha, \tilde{\boldsymbol{K}} > \boldsymbol{0} \tag{15}$$

is identified using the input-to-state stability approach.[17,18] The procedure for finding $\boldsymbol{R}$ is similar as in Chung et al.[6]

Remark 2. The requirement that $\boldsymbol{Q}$ and $\boldsymbol{R}$ are positive definite delivers the following conditions for $\tilde{\boldsymbol{K}}$, $\boldsymbol{K}_{\mathrm{p}}$ and $\boldsymbol{K}_{\mathrm{d}}$:

- $\tilde{\boldsymbol{K}}$, $\boldsymbol{K}_{\mathrm{p}}$ and $\boldsymbol{K}_{\mathrm{d}} \geq \boldsymbol{0}$,
- $\boldsymbol{K}_{\mathrm{d}}^2 \geq 2\boldsymbol{K}_{\mathrm{p}}$.

https://doi.org/10.1017/S0263574719000547 Published online by Cambridge University Press

Theorem 1 shows that the adaptive controller along with the matrices given by $\boldsymbol{Q}$ and $\boldsymbol{R}$ leads to a robust-optimal solution. Theorem 2 explains how to choose the control parameters that will satisfy the maximum allowed joint errors at steady state. For the quantitative performance analysis, we define the maximum error $|\boldsymbol{x}_{\text{perf}}|$ that is allowed in the steady state. $\tilde{\boldsymbol{K}}$ is assumed to be scalar for the sake of simplicity.

Theorem 2. *For the control law (7) with the conditions given in Remark 2, the performance limitation $|\boldsymbol{x}_{\text{perf}}|$ is provided as*[4]

$$|\boldsymbol{x}_{\text{perf}}| \leq \frac{2\boldsymbol{SB}}{\lambda_{\min}}|\phi_{\max}|, \tag{16a}$$

where

$$\lambda_{\min} = \lambda_{\min}\big(\boldsymbol{Q} + (2a - \tilde{K})\boldsymbol{SBB}^T\boldsymbol{S}\big). \tag{16b}$$

Proof. Let the Lyapunov function for the game-algebraic Riccati equation along with worst-case disturbance (11) be given by

$$V(\boldsymbol{x}) = \frac{1}{2}\boldsymbol{x}^T\boldsymbol{S}\boldsymbol{x}. \tag{17}$$

Using Eq. (8), the first derivative of Eq. (17) delivers

$$\dot{V} = \frac{1}{2}\boldsymbol{x}^T(\boldsymbol{A}^T\boldsymbol{S} + \boldsymbol{SA})\boldsymbol{x} + \boldsymbol{x}^T\boldsymbol{SB}\hat{\phi} - \boldsymbol{x}^T\boldsymbol{SB}\phi. \tag{18}$$

Using Eqs. (11) and (15) with scalar $\tilde{K}$, we obtain

$$\dot{V} = -\frac{1}{2}\boldsymbol{x}^T\big(\boldsymbol{Q} + (2a - \tilde{K})\boldsymbol{SBB}^T\boldsymbol{S}\big)\boldsymbol{x} - \boldsymbol{x}^T\boldsymbol{SB}\phi. \tag{19}$$

The first term is negative if $2a > \tilde{K}$, which is obvious from Eq. (15). With Eq. (16b), we get

$$\dot{V} \leq -\frac{1}{2}\lambda_{\min}\boldsymbol{x}^T\boldsymbol{x} - \boldsymbol{x}^T\boldsymbol{SB}\phi. \tag{20}$$

Using that $\dot{V} < 0$, we obtain a performance limitation

$$|\boldsymbol{x}_{\text{perf}}| \leq \frac{2\boldsymbol{SB}}{\lambda_{\min}}|\phi_{\max}|.$$

To summarize, the state vector $|\boldsymbol{x}|$ will decrease until $|\boldsymbol{x}| \leq |\boldsymbol{x}_{\text{perf}}|$ because of the performance limitation explained in Theorem 2.

3.2. Modified desired trajectory

The joint errors will not exceed the maximum allowed error $|\boldsymbol{x}_{\text{perf}}(2)| = |\boldsymbol{e}_{\text{perf}}|$ in steady state if the control parameters are selected according to Eq. (16a). However, Eq. (16a) might not be satisfied because the controller does not consider input constraints,

$$|\boldsymbol{\tau}| < |\overline{\boldsymbol{\tau}}|.$$

For the trajectory scaling, we selected the state error $\boldsymbol{e}$ as a design feature, since the proposed adaptive controller offers quantitative performance analysis. The desired trajectory is modified whenever $\boldsymbol{e}$ exceeds a maximum allowed values at steady state. $|\boldsymbol{x}_{\text{perf}}|$ is a function of the system dynamics $\phi(\boldsymbol{q}, \dot{\boldsymbol{q}}, \ddot{\boldsymbol{q}})$ and input torques are dependent on the estimate of ϕ. So, to deal with the unknown saturation, the speed of the desired trajectory should be compromised whenever the error at steady state exceeds the maximum allowed $|\boldsymbol{e}_{\text{perf}}|$. Next we explain how to modify the desired trajectory by making the path a function of a variable θ rather than time.[1,12] Intuitively, the trajectory is tracked slower when the motor drives cannot deliver the required current/torque. At times when the torque requirements are low, the speed of the trajectory can be increased to achieve the task in a prescribed span of time. A scalar differential equation is proposed to perform a variable speed scaling for the desired trajectory.

https://doi.org/10.1017/S0263574719000547 Published online by Cambridge University Press

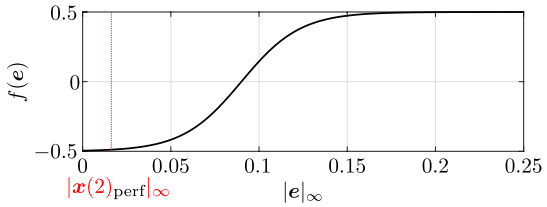


Fig. 2. User-defined specification for $f(\boldsymbol{e})$.

Trajectory scaling: Given a desired trajectory $x_d(\theta)$, where $\theta = t$ only when the torque required for generating the desired motion does not saturate $|\bar{\tau}|$. Otherwise,

$$\frac{d\theta}{dt} = 0.5 - f(\boldsymbol{e}) + g(\theta, t), \quad \theta(t_0) = 0, \tag{21}$$

where

$$f(\boldsymbol{e}) = 0.5 \tanh\left(K_1(|\boldsymbol{e}(t)|_\infty - x_{\text{off}})\right),$$
$$g(\theta, t) = K_2(t - \theta),$$

where $|\boldsymbol{e}(t)|_\infty = |\boldsymbol{x}(2)_{\text{perf}}|_\infty$ is a scalar representing the maximum joint error, K_1 and K_2 are positive gains and x_{off} is an offset. The function $f(\boldsymbol{e})$ can be derived from Fig. 2 using curve-fitting technique. From the above differential equation, there are three conditions as follows:

1. If $|\boldsymbol{e}(t)|_\infty \leq |\boldsymbol{x}(2)_{\text{perf}}|_\infty$ for all t, then $\theta = t$ because $f(\boldsymbol{e}) = -0.5$ and $g(\theta, t) = 0$.
2. If $|\boldsymbol{e}(t)|_\infty > |\boldsymbol{x}(2)_{\text{perf}}|_\infty$, then $\theta < t$ because $-0.5 < f(\boldsymbol{e}) \leq 0.5$ thus decreasing the speed of trajectory.
3. If $|\boldsymbol{e}(t)|_\infty \leq |\boldsymbol{x}(2)_{\text{perf}}|_\infty$ and $\theta(t) < t$, then

$$\theta(t) = t + \theta(t_0)e^{-K_2 t},$$

where t_0 is the time instant where $|\boldsymbol{e}(t)|_\infty > |\boldsymbol{x}(2)_{\text{perf}}|_\infty \rightarrow |\boldsymbol{e}(t)|_\infty \leq |\boldsymbol{x}(2)_{\text{perf}}|_\infty$.

The function $f(\boldsymbol{e})$ returns an output in the range of -0.5 to 0.5. If the error in the joint angle is above the allowed maximum error during the steady state, θ will slow down according to the magnitude of the error. Once the trajectory is slowed down enough that the adaptive control can follow the desired trajectory, $f(\boldsymbol{e}) \rightarrow -0.5$. The term $g(\theta, t)$ always tries to reduce the error between θ and t. Depending on the value of the gain K_2, θ will move faster to approach t. The functions $f(\boldsymbol{e})$ and $g(\theta, t)$ have conflicting objectives. The former tries to slow down the trajectory and the latter tries to increase the speed of trajectory. The domination of $f(\boldsymbol{e})$ depends on the speed of desired trajectory. If $\tau_{\text{in}} > |\bar{\tau}|$ for most part of the trajectory tracking, then $g(\theta, t)$ will not have enough time to force $\theta \rightarrow t$, and one complete circular rotation would take more time compared to the original trajectory. Although the trajectory modification improves both the transient and steady-state performance, however, if the starting position of the end effector is far away from the desired trajectory, there will be peaking.

The state-of-the-art methods use time-optimal control methods.[12,13] However, these techniques require knowledge about the input saturation.

Remark 3. The function $f(\boldsymbol{e})$ can be selected differently, for example, a ramp function or a step function. The only conditions are that $f(\boldsymbol{e}) = -0.5$ if $|e|_\infty \leq |\boldsymbol{x}_{\text{perf}}(2)|_\infty$ and $f(\boldsymbol{e}) = 0.5$ if $|e|_\infty >> |\boldsymbol{x}_{\text{perf}}(2)|_\infty$. Eq. (21) can be customized and velocities of the joint errors can also be included in defining the trajectory modification.

Remark 4. The trajectory scaling method devised in this section is not specific to the adaptive controller (7) because the method only modifies the reference signal and not the controller.

https://doi.org/10.1017/S0263574719000547 Published online by Cambridge University Press

3.3. Improve transient response

The trajectory scaling explained in the previous subsection improves both the transient and steady-state performance as it will be evident in Section 4. But there might be a peaking effect if the initial conditions for the joint angles are not in the region of attraction, that is, $|\boldsymbol{e}(0)|_\infty >> |\boldsymbol{x}(2)_{\text{perf}}|_\infty$.

To improve the performance in terms of joint errors, we will first discuss the cause of the peaking effect. For the proposed adaptive controller, a high gain a for the control Eq. (7) is required to remove the mismatch as quickly as possible and thus have a system with performance similar to Eq. (3). To show the necessity of high gain for the controller gains, we use the Bellman equation[16]

$$\dot{V} + \frac{1}{2}\left(\boldsymbol{x}^T\boldsymbol{Q}\boldsymbol{x} + \boldsymbol{u}^T\boldsymbol{R}\boldsymbol{u} - \gamma^2\boldsymbol{d}^T\boldsymbol{d}\right) = 0. \tag{22}$$

Using Eq. (10), we can rewrite the Bellman equation in input-to-state-stable form as

$$\dot{V} \leq -\frac{1}{2}\lambda_{Q_k}\boldsymbol{x}^T\boldsymbol{x} + \frac{1}{2}\gamma^2\boldsymbol{d}^T\boldsymbol{d} := -\gamma_1||\boldsymbol{x}||^2 + \gamma_2||\boldsymbol{d}||^2 \quad \gamma_1, \gamma_2 > 0, \tag{23}$$

where λ_{Q_k} is the minimum eigenvalue of the matrix $\boldsymbol{Q} + \boldsymbol{K}^T\boldsymbol{K}$. From the above equation, we can also set the maximum allowed steady-state error as explained in Section 3.1. Integrating the previous equation:

$$||\boldsymbol{x}||_2^2 \leq \frac{2}{\lambda_{Q_k}}V(0) + \frac{\gamma^2}{\lambda_{Q_k}}||\boldsymbol{d}||_2^2, \tag{24}$$

where $-\int_0^\infty \dot{V}\mathrm{d}t = -V(\infty) + V(0) \leq V(0)$. Under the assumption that at any time the cost function is given by

$$V(0) = \frac{1}{2}\boldsymbol{x}^T(0)\boldsymbol{S}\boldsymbol{x}(0),$$

the $\mathcal{L}_2$ norm of states is given by

$$||\boldsymbol{x}||_2^2 \leq \frac{\lambda_S}{\lambda_{Q_k}}||\boldsymbol{x}(0)||^2 + \frac{\gamma^2}{\lambda_{Q_k}}||\boldsymbol{d}||_2^2, \tag{25}$$

where λ_S is the maximum eigenvalue of $\boldsymbol{S}$. From the above result, it is evident that the joint error decreases as we increase the controller gains λ_{Q_k}. Also, the offset in the steady state reduces with higher controller gain.

We have shown quantitatively that high gains are essential to achieve better performance regarding tracking error. Next, we will present the adverse effect of high gains, which is also called peaking effect in literature. High gains introduce high-frequency oscillations during the transient phase, which might make the system unstable. Some of this influence is reduced naturally because of the input saturation. Also, the motor drives have a first-order response that limits high-frequency torque. The oscillations in transient-response are because of the derivative of the input applied to the system:

$$\dot{\boldsymbol{u}} = -\boldsymbol{K}\dot{\boldsymbol{x}}. \tag{26}$$

After some computation, the $\mathcal{L}_2$ norm of input $\boldsymbol{u}$ is given by

$$||\dot{\boldsymbol{u}}||_2^2 \leq \lambda_{k_{\max}}||\boldsymbol{A}\boldsymbol{x} + \boldsymbol{B}\tilde{\phi}||_2^2, \tag{27}$$

where $\lambda_{k_{\max}}$ is the maximum eigenvalue of $\boldsymbol{K}^T\boldsymbol{K}$. From Eq. (26), we conclude that the oscillations, which deteriorate the transient response, increase with high controller gain $\boldsymbol{K}$, joint errors and the mismatch. Of course, once the system reaches steady state and the mismatch $\tilde{\phi} \to \boldsymbol{0}$, the effect of oscillations is minimal and can be ignored.

To summarize, we need a low controller gain during the transient response because the initial conditions are usually unknown and can be anywhere in the workspace of the robot end effector. Next, a couple of techniques for the improvement of the transient response are presented.

https://doi.org/10.1017/S0263574719000547 Published online by Cambridge University Press

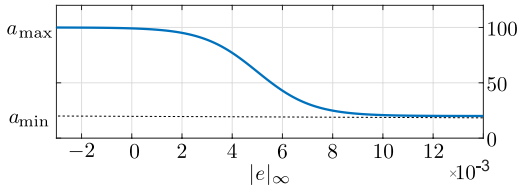


Fig. 3. Specifications for the gain scheduling used in the results.

3.3.1. Procedure 1. This procedure is inspired from Na et al.,[24] where a model-reference adaptive control is used. An extra term is added to the input torque, which depends on the filtered values of the states.

Let $\boldsymbol{x}_{\mathrm{f}}$ is the filtered values of states,

$$k\dot{\boldsymbol{x}}_{\mathrm{f}} + \boldsymbol{x}_{\mathrm{f}} = \boldsymbol{x} \tag{28}$$

and

$$\boldsymbol{E} = \boldsymbol{A}\boldsymbol{x}_{\mathrm{f}} - \frac{\boldsymbol{x} - \boldsymbol{x}_{\mathrm{f}}}{k}. \tag{29}$$

By adding the term $\boldsymbol{E}$ in the input torque, the state space representation of Eq. (6) is given by

$$\dot{\boldsymbol{x}} = \boldsymbol{A}\boldsymbol{x} + \boldsymbol{B}\tilde{\phi} + \boldsymbol{E}. \tag{30}$$

The above equation can be written as

$$\dot{\boldsymbol{x}} = \boldsymbol{A}\boldsymbol{x} + \boldsymbol{B}(\tilde{\phi} - \tilde{\phi}_f). \tag{31}$$

Considering the new system dynamics, the oscillations in the systems can be related to

$$||\dot{\boldsymbol{u}}||_2^2 \leq \lambda_{k_{\max}} ||\boldsymbol{A}\boldsymbol{x} + \boldsymbol{B}(\tilde{\phi} - \tilde{\phi}_f)||_2^2. \tag{32}$$

As it is clear that $\dot{\boldsymbol{u}}$ is reduced because of the factor $\tilde{\phi} - \tilde{\phi}_f$. The value of k is selected as low as possible such as to avoid oscillations.

3.3.2. Procedure 2. To reduce the oscillation, one method is to use small values of gains a during the transient response. For that purpose, after selecting minimum and maximum values of a, the gains for the controller can be adjusted as follows:

Let

$$a(\boldsymbol{x}) = \frac{a_{\max} - (a_{\max} - a_{\min})}{1 + \sigma_1^{(|e|_\infty - \sigma_2)}}, \tag{33}$$

the values for σ_1 and σ_2 can be easily identified using Fig. 3.

Theorem 3. *The system* (6) *and control law* (7)*, along with the modified gain* $a(\boldsymbol{x})$ *of* (33)*, result in a stable closed-loop system.*

Proof. The stability of the modified controller is easily verified using Eq. (22). The control vector $\boldsymbol{K}$ is now a function of the states, but there are upper and lower bounds because of $a_{\max}$ and $a_{\min}$. We get

$$\dot{V} = -\frac{1}{2}\boldsymbol{x}^T\big(\boldsymbol{Q} + \boldsymbol{K}^T(\boldsymbol{e})\boldsymbol{K}(\boldsymbol{e})\big) - \frac{1}{2}\gamma^2\boldsymbol{d}^T\boldsymbol{d}. \tag{34}$$

Because $\boldsymbol{K}(\boldsymbol{e})$ is bounded, $\dot{V}$ is always negative with respect to the states if condition (16a) is satisfied for all $a(\boldsymbol{x})$.[33]

The controller gain $\boldsymbol{K}$ becomes a constant as $\boldsymbol{x}$ approaches to zero. More details about the state-dependent controller gains are available in refs. [21, 22].

https://doi.org/10.1017/S0263574719000547 Published online by Cambridge University Press

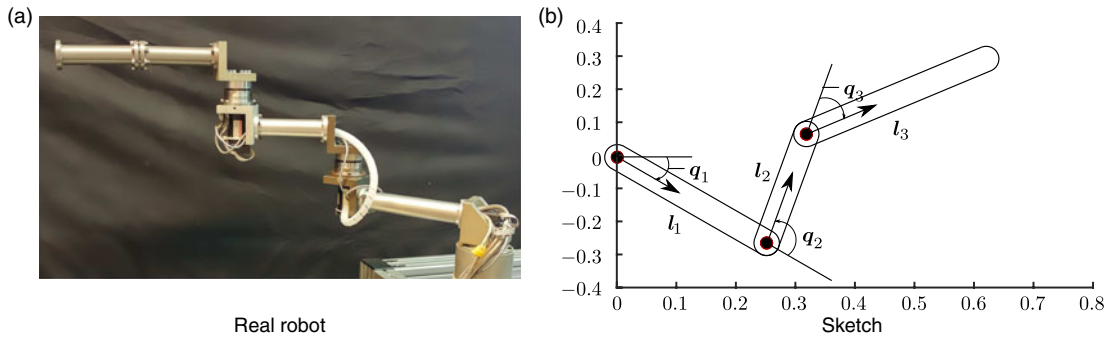


Fig. 4. A 3-DoF manipulator used in experiments. The lengths are $l_1 = 0.305\ m$, $l_2 = 0.225\ m$ and $l_3 = 0.305\ m$.

Remark 5. A simple filter can be applied on the input torque to get slight improvement in terms of noise. The oscillations in the system are because of the $\dot{\hat{\phi}}$ which is used in finding the input torque. To show this effect, we have

$$\dot{\boldsymbol{\tau}}_{\text{in}} = \ddot{\hat{\boldsymbol{\phi}}} + \dddot{\boldsymbol{q}}_{\text{d}} + \boldsymbol{A}\dot{\boldsymbol{x}}, \tag{35}$$

$$\dot{\boldsymbol{\tau}}_{\text{in}} \leq |\ddot{\hat{\boldsymbol{\phi}}}| + |\dddot{\boldsymbol{q}}_{\text{d}}| + |\boldsymbol{A}^2\dot{\boldsymbol{x}} + \boldsymbol{AB}\tilde{\boldsymbol{\phi}}|. \tag{36}$$

For the experiments performed in this paper, the low-pass filter is not used because of the power supply acting as a filter. In the end, a systematic and intuitive procedure is devised to find the control parameters, analytically or numerically.

3.4. Auto-tuning for the controller

This subsection explains a systematic and intuitive strategy to find the control parameters for the controller (7).

1. Evaluate the minimum values for the control parameters using Eq. (16a) that satisfy the condition for the allowed maximum joint error at steady state.
2. Find the values of $\boldsymbol{K}_{\text{p}}$ and $\boldsymbol{K}_{\text{d}}$ satisfying a performance criterion such as settling time and rise time.
3. Choose a such that the value of the pole of[3]

$$\dddot{\tilde{\boldsymbol{\phi}}} + a\ddot{\tilde{\boldsymbol{\phi}}} = \boldsymbol{0}$$

is 3–5 times higher than the poles of (3).

The intuition for the above procedure is that the PD gains will perform in a deterministic way by choosing a proper rise time, settling time, and so on. The PD controller will perform linearly only if the mismatch is removed. For that reason, the pole location for the convergence of mismatch to zero (a) must be faster than the PD gains ($\boldsymbol{K}_{\text{p}}$ and $\boldsymbol{K}_{\text{d}}$). Finally, to compensate for the peaking effect during transient phase, a is selected as a variable with upper and lower bounds (see Section 3.2).

4. Simulations and Experiments

A three-degree-of-freedom (3-DoF) planar robot is used to validate the proposed controller in both simulations and experiments. For experiments, 10-ampere Maxon drives along with 150-watt motors are used (Fig. 4). The desired end-effector trajectory $\boldsymbol{q}_d$ is a circle in the first quadrant of the x–y plane with radius 0.24 m and center $0.3\hat{x}$ m $+ 0.3\hat{y}$ m. The values for the controller gains are $\boldsymbol{K}_{\text{p}} = 40\boldsymbol{I}$, $\boldsymbol{K}_{\text{d}} = 400\boldsymbol{I}$, $a = 80$ and $|\boldsymbol{e}_{\text{perf}}|_\infty = 0.01$ rad. The end effector starts at $\hat{x}$ 0.83 m. The dynamical equations of the 3-DoF robot manipulator used in experiments are calculated from the real robot; see Table I. Since, the adaptive controller is model-free, the dynamics are only used for simulations.

4.1. Simulations

The simulation results are divided into three parts. The objective of the first result is to show that using Eq. (16a), the joint error at steady state is always less than $|\boldsymbol{e}_{\text{perf}}|_\infty = 0.01$ rad/s. Figure 5

https://doi.org/10.1017/S0263574719000547 Published online by Cambridge University Press

Table I. The dynamical equations of 3-DoF planar robot.

Var.	**Equivalent**
$M(1,1)$	$1.04+0.08\cos(q_2+q_3)+0.34\cos(q_2)+0.05\cos(q_3)$
$M(1,2)$	$0.43+0.04\cos(q_2+q_3)+0.17\cos(q_2)+0.05\cos(q_3)=M(2,1)$
$M(1,3)$	$0.17+0.04\cos(q_2+q_3)+0.023\cos(q_3)=M(3,1)$
$M(2,2)$	$0.43+0.05\cos(q_3)$
$M(2,3)$	$0.17+0.03\cos(q_3)=M(3,2)$
$M(3,3)$	0.17
$N(1,1)$	$-0.17\sin(q_2)\dot{q}_2^2-0.04\sin(q_2+q_3)\dot{q}_2^2-0.03\sin(q_3)\dot{q}_3^2-0.04\sin(q_2+q_3)\dot{q}_3^2$ $-0.34\sin(q_2)\dot{q}_1\dot{q}_2-0.08\sin(q_2+q_3)\dot{q}_1\dot{q}_2-0.05\sin(q_3)\dot{q}_1\dot{q}_3$ $-0.08\sin(q_2+q_3)\dot{q}_1\dot{q}_3-0.05\sin(q_3)\dot{q}_2\dot{q}_3-0.08\sin(q_2+q_3)\dot{q}_2\dot{q}_3$
$N(1,2)$	$0.17\sin(q_2)\dot{q}_1^2+0.04\sin(q_2+q_3)\dot{q}_1^2-0.03\sin(q_3)\dot{q}_3^2-0.05\sin(q_3)\dot{q}_1\dot{q}_3$ $-0.05\sin(q_3)\dot{q}_2\dot{q}_3$
$N(1,3)$	$0.028\sin(q_3)\dot{q}_1^2+0.03\sin(q_3)\dot{q}_2^2+0.04\sin(q_2+q_3)\dot{q}_1^2+0.05\sin(q_3)\dot{q}_1\dot{q}_2$
$F(i,j)$	$2.6\times10^4\ \ \forall\, i=j$
$F(i,j)$	$0\ \ \forall\, i\neq j$

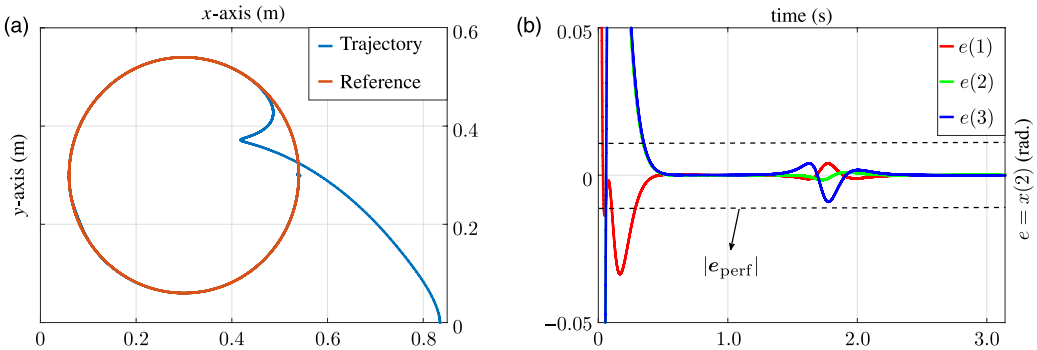


Fig. 5. Simulation: tracking without input constraints: (a) position of the end effector in Cartesian coordinates; (b) joint errors.

shows that the error at steady state is much lower than 0.01 rad/s for all time during steady state. For one complete rotation of the end effector, the desired trajectory requires 3.14 s. Here the assumption is that the torque requirements for the desired trajectory are lower than the saturation.

The second set of simulations shows how the torque saturation affects the trajectory tracking. We have increased the speed of the desired path until input saturation is reached, and thus the manipulator could not follow the trajectory for most of the desired trajectory as shown in Fig. 6(a). The desired trajectory span was 1.62 s for one complete rotation. After applying the path scaling, the trajectory slowed down in the region where the input torque requirement is higher than the saturation Fig. 6(b). The modified desired trajectory makes sure that the error is much lower compared to the previous results. The parameters for the trajectory modification (21) are evaluated using Fig. 2. Figure 7 shows that the parameter θ, which ideally is equal to time, slowed down during the first 1000 ms because of the function $f(\boldsymbol{e})$. In the last half of the desired trajectory, the function $g(\theta, t)$ reduces the difference between θ and t. At the end of one complete circle, the total time is equal for both the trajectories in Fig. 6, as evident from Fig. 7.

The third result provides the improvement of the transient response by using the two techniques of Section 3.3. Figure 8 shows the effect of variable gain to improve the transient response. The maximum and minimum values for the parameter a are 80 and 20, respectively, as in Fig. 3.

4.2. Experimental results

The adaptive controller includes all the uncertainties and disturbance in the vector ϕ, and as long as ϕ is bounded, the controller will force the system to follow the desired trajectory with an accuracy of 0.01 rad. Figure 9 shows results of two experiments with the same desired trajectory but with different

https://doi.org/10.1017/S0263574719000547 Published online by Cambridge University Press

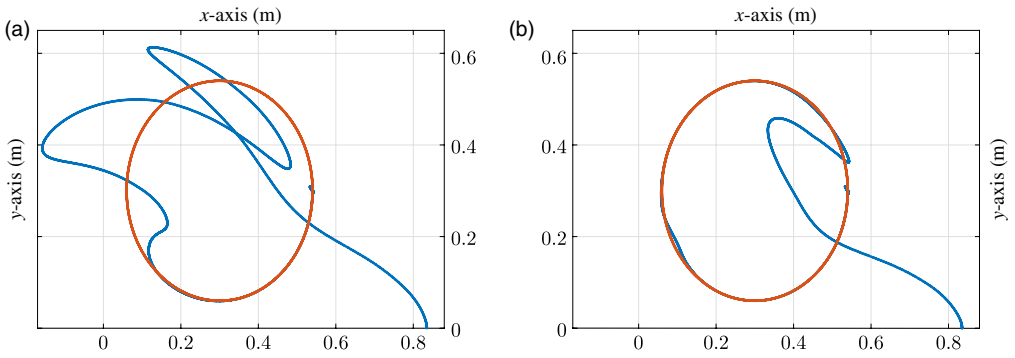


Fig. 6. Simulation: trajectory in the presence of input constraints. (a) Without scaling and (b) with scaling.

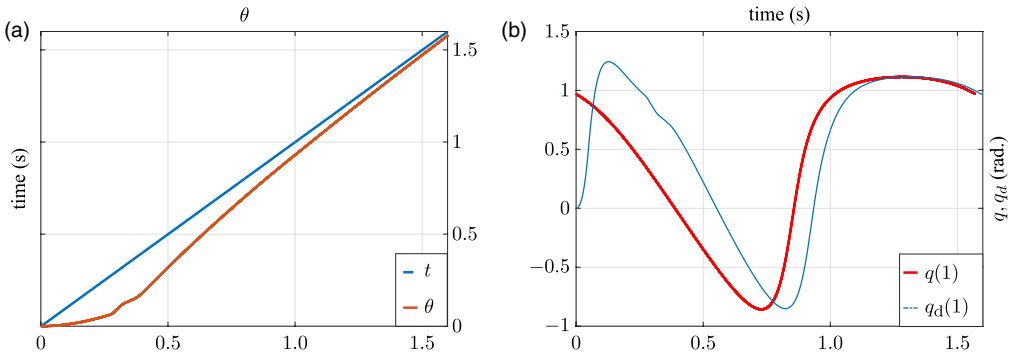


Fig. 7. Simulation: comparison of time t and θ. (a) t and θ; (b) q and q_d.

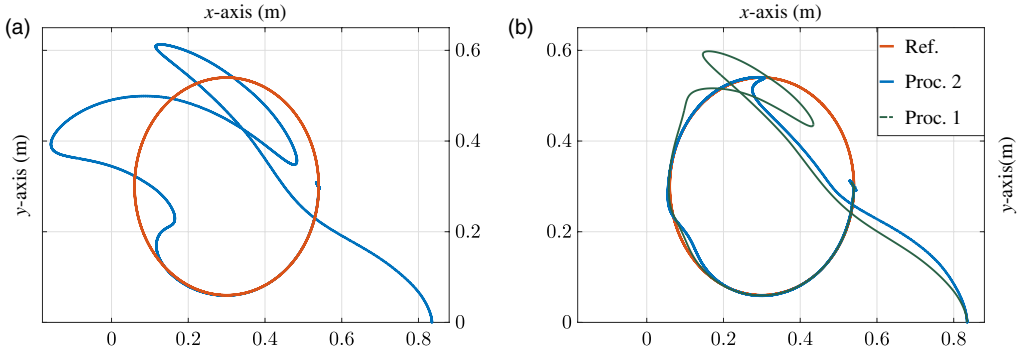


Fig. 8. Simulation: (a) without gain adjustment. (b) Gain adjustment with $a = 20 - 80$ using (33).

speeds. The first experiment, Fig. 9 (a-blue and b) satisfies the $|\boldsymbol{e}_{\text{perf}}|_\infty = 0.01$ bound because the torques for the desired trajectory are less than the saturation. This condition is not satisfied if the torque saturation is lower than the required torque as evident in Fig. 9 (a-green and c). The desired trajectory took 3.1/1.2 s for one complete rotation for blue/green trajectories. To make sure that the end effector follows the orbit of the desired trajectory, the second experiment is improved by modifying the desired trajectory. Figure 10 (a-blue and b) shows that the performance limitations are now satisfied but the total time required for the circular trajectory is higher than the original time Fig. 9 (c). The transient response is further improved by using the variable gain technique from Section 3 as shown in Fig. 9 (a-green).

5. Conclusion

Robust optimality of the first-order adaptive controller is evaluated using $\mathcal{H}_\infty$ technique. The stability is proved by using the inverse-optimal method, where the matrices for the optimized cost function are identified using the adaptive controller. To compensate for the unknown torque saturation, a solution

https://doi.org/10.1017/S0263574719000547 Published online by Cambridge University Press

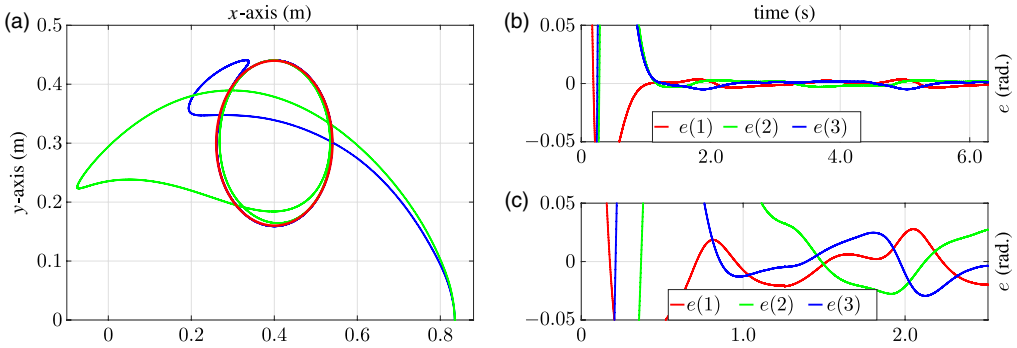


Fig. 9. Experiment: (a) trajectory of the end effector; (b) shows that the performance limitation is satisfied by the blue trajectory in (a). (c) represents the error in the joint angles for the green trajectory in (a).

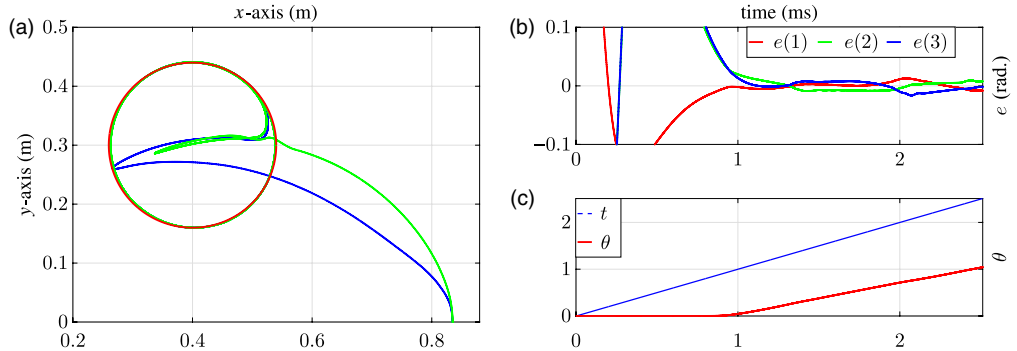


Fig. 10. Experiments: (a) the desired trajectory took 1.2 s for one complete rotation for both trajectories. (b) shows that the performance limitation is satisfied by the blue trajectory in (a). (c) represents the difference between θ (red) and t (blue).

is proposed that modifies the speed of the desired trajectory such that the error in the joint angles remains within certain bounds at steady state. For the transient response improvement, two methods are discussed that can be used to improve the high-frequency noise and peaking effect during the transient phase. And lastly, an intuitive procedure for the identification of the minimum allowed control parameters is formalized.

Acknowledgments

The research leading to these results has received funding from Higher Education Commission of Pakistan under the Faculty Development Program "Universities of Engineering, Science and Technology Program (UESTP) – Germany (57076459)."

References

1. S. S. Pchelkin, A. S. Shiriaev, A. Robertsson, L. B. Freidovich, S. A. Kolyubin, L. V. Paramonov and S. V. Gusev, "On orbital stabilization for industrial manipulators: Case study in evaluating performances of modified PD+ and inverse dynamics controllers," *IEEE Trans. Control Syst. Technol.* **25**(1), 101–117 (2017).
2. Y. Feng, X. Yu and Z. Man, "Non-singular terminal sliding mode control of rigid manipulators," *Automatica* **38**(12), 2159–2167 (2002).
3. R. Hayat and M. Buss,"Model identification for robot manipulators using regressor-free adaptive control," *UKACC 11th International Conference on Control (UKACC)* (2016) pp. 1–7.
4. R. Hayat, M. Leibold and M. Buss, "Robust-adaptive controller design for robot manipulators using the $\mathcal{H}_\infty$ approach," *IEEE Access* **6**, 51626–51639 (2018).
5. J. Park and W. K. Chung,"Analytic nonlinear $\mathcal{H}_\infty$ inverse-optimal control for Euler–Lagrange system," *IEEE Trans. Robot. Automat.* **16**(6), 847–854 (2000).
6. Y. Choi, W. K. Chung and I. H. Suh, "Performance and $\mathcal{H}_\infty$ optimality of PID trajectory tracking controller for Lagrangian systems," *IEEE Trans. Robot. Automat.* **17**(6), 857–869 (2001).
7. M. J. Kim, Y. Choi and W. K. Chung, "Bringing nonlinear $\mathcal{H}_\infty$ optimality to robot controllers," *IEEE Trans. Robot.* **31**(3), 682–698 (2015).

https://doi.org/10.1017/S0263574719000547 Published online by Cambridge University Press

8. J. J. Slotine and W. Li, "On the adaptive control of robot manipulators," *Int. J. Robot. Res.* **6**(3), 49–59 (1987).
9. C. Y. Kai and A. C. Huang, "A regressor-free adaptive controller for robot manipulators without Slotine and Li's modification," *Robotica* **31**(7), 1051–1058 (2013).
10. A. C. Huang, S. C. Wu and W. F. Ting, "A FAT-based adaptive controller for robot manipulators without regressor matrix: theory and experiments," *Robotica* **24**(2), 205–210 (2006).
11. A. S. Shiriaev, L. B. Freidovich and S. V. Gusev, "Transverse linearization for mechanical systems with several passive degrees of freedom with applications to orbital stabilization," *American Control Conference*(2009) pp. 3039–3044.
12. D. Verscheure, B. Demeulenaere, J. Swevers, J. De Schutter and M. Diehl, "Time-optimal path tracking for robots: A convex optimization approach," *IEEE Trans. Automat. Control.* **54**(10), 2318–2327 (2009).
13. J. E. Bobrow, S. Dubowsky and J. S. Gibson, "Time-optimal control of robotic manipulators along specified paths," *Int. J. Robot. Res.* **4**(3), 3–17 (1985).
14. Hassan K. Khalil, ' '*Nonlinear Systems*," (Prentice-Hall, NJ, 1996).
15. J. J. Craig, "*Introduction to Robotics: Mechanics and Control*," (Pearson Prentice Hall, Upper Saddle River, NJ, 2005).
16. F. L. Lewis, D. Vrabie and V. L. Syrmos, "*Optimal control*," vol. 3 (Wiley, Hoboken, NJ, 2012).
17. E. D. Sontag and Y. Wang, "On characterizations of the input-to-state stability property," *Syst. Control Lett.* **24**(5), 351–359 (1995).
18. E. D. Sontag, "Input to state stability: Basic concepts and results,"**In**: *Nonlinear and Optimal Control Theory* (2008) pp. 163–220.
19. C. Kim and K. Lee, "Robust control of robot manipulators using dynamic compensators under parametric uncertainty," *Int. J. Innov. Comput. Inf. Control* **7**(7), 4129–4137 (2011).
20. A. S. Shiriaev, L. B. Freidovich and I. R. Manchester, "Can we make a robot ballerina perform a pirouette? Orbital stabilization of periodic motions of underactuated mechanical systems," *Ann. Rev. Control* **32**(2), 200–211 (2008).
21. J. R. Cloutier, C. N. D'Souza and C. P. Mracek, "Nonlinear Regulation and Nonlinear H Control via the State-Dependent Riccati Equation Technique: Part 1, Theory," *Proceedings of the First International Conference on Nonlinear Problems in Aviation and Aerospace* (1996) pp. 117–130.
22. X. Xu, J. J. Zhu and P. Zhang, "The optimal solution of a non-convex state-dependent LQR problem and its applications," *PloS One* **9**(4), e94925 (2014).
23. H. A. Modares, F. L. Lewis and M.-B. N. Sistani, "Online solution of nonquadratic two-player zero-sum games arising in the H control of constrained input systems," *Int. J. Adapt. Control Signal Process.* **28**(3–5), 232–254 (2014).
24. J. Na, G. Herrmann and K. Zhang, "Improving transient performance of adaptive control via a modified reference model and novel adaptation," *Int. J. Robust Nonlin. Control* **27**(8), 1351–1372 (2017).
25. T. Basar and G. J. Olsder, "Dynamic noncooperative game theory," *SIAM* **23** (1999).
26. M. N. Mahyuddin, S. G. Khan and G. Herrmann, "A novel robust adaptive control algorithm with finite-time online parameter estimation of a humanoid robot arm," *Robot. Auton. Syst.* **62**(3), 294–305 (2014).
27. J. J.-B. M. Ahanda, J. B. Mbede, A. Melingui and B. Essimbi, "Robust adaptive control for robot manipulators: Support vector regression-based command filtered adaptive backstepping approach," *Robotica*. 1–19 (2017).
28. B. S. Chen, T. S. Lee and J. H. Feng, "A nonlinear $\mathcal{H}_\infty$ control design in robotic systems under parameter perturbation and external disturbance," *Int. J. Control* **59**(2), 439–461 (1994).
29. K. Ogata, *Modern Control Engineering*, 5th edition (Prentice Hall, Upper Saddle River, NJ, 2009).
30. D. Zhang and B. Wei, "Design, analysis and modelling of a hybrid controller for serial robotic manipulators," *Robotica* **35**(9), 1888–1905 (2017).
31. M. A. Arteaga-Pérez and A. Gutiérrez-Giles, "On the GPI approach with unknown inertia matrix in robot manipulators," *Int. J. Control* **87**(4), 844–860 (2014).
32. J. Han, "From PID to active disturbance rejection control," *IEEE Trans. Ind. Electron.* **56**(3), 900–906 (2009).
33. T. Cimen, "State-Dependent Riccati Equation (SDRE) control: A survey," *IFAC Proceedings Volumes: Elsevier* **41**(2), 3761–3775 (2008).

https://doi.org/10.1017/S0263574719000547 Published online by Cambridge University Press